Alkynes in covalent enzyme inhibitors: down the kinetic rabbit hole

Mons, E.


Kinase
IC50

Chapter 7

Happily Ever After:
A Summary and Discussion

1. Summary

Once upon a time... irreversible covalent inhibitors were discovered by accident and actively avoided in drug development. In ***Chapter 1***, a historic perspective on the development of irreversible covalent inhibitors illustrated how compounds with potential covalent binding modes were excluded from industrial drug development programs despite the prevalence of safe blockbuster drugs that were later found to have an irreversible covalent binding mode. The past two decades marked a resurgence of irreversible covalent drugs for protein targets that require prolonged inhibition for therapeutic effect, and led to the development of targeted covalent inhibitors (TCIs) that have a strategically placed electrophilic moiety. TCIs were instrumental in overcoming acquired resistance to noncovalent inhibitors (e.g. third-generation inhibitor **osimertinib** (Tagrisso, AZD9291) targeting EGFR mutants over wild-type), and some TCIs are first-in-class drugs tackling previously 'undruggable' oncogenes (e.g. **sotorasib** (Lumakras, AMG 510) and **adagrasib** (Krazati, MRTX849) targeting $KRAS^{G12C}$).[1-2] Novel thiol-reactive warheads that balance chemical reactivity with superior target selectivity have an important role to further improve the safety profiles. Acetylenes are a privileged structural motif in drug discovery, and terminal alkynes have been extensively used as bioorthogonal Click handles in chemical biology tools – owing to their selective reactivity with azides in the copper-catalyzed azide–alkyne cycloaddition (CuAAC) while displaying a low propensity of spontaneous engagement in covalent adducts with cellular components. Aside from the CuAAC reaction forming a triazole and the radical-mediated thiol–yne coupling (TYC) forming an *anti*-Markovnikov-type thiovinyl, covalent adduct formation with acetylenes requires promotion by metabolic activation, isomerization to a reactive allenic intermediate, metal catalysis, or chemical modification of the acetylene to generate a reactive electron-deficient alkyne. In 2013, the Ovaa[3] and Mootz[4] groups independently discovered that Ub(l)-**Prg** – intended as building blocks for protease-resistant nonhydrolyzable substrates – can form a covalent Markovnikov-type thiovinyl adduct with catalytic cysteine residues of Ub(l) proteases. This serendipitous discovery challenged the paradigm that nonactivated alkynes are 'inert' towards cellular components under physiological conditions but covalent adducts were only detected if the propargylated peptide had a relatively large recognition element (>1.8 kDa) and substituents on the propargylamide mitigated adduct formation with UCHL3. In this dissertation, we explored the scope and versatility of the newly-discovered *in situ* thiol–alkyne reaction: from nonactivated alkyne warheads in irreversible covalent small molecule drugs to substituted propargyl analogues in chemical tools.

Part 1: Theoretical Framework for the Evaluation of Covalent Inhibitors

There are many indirect methods to deduce a covalent binding mode from (time-dependent) disappearance of intact drug and/or unbound protein, but experimental detection of the covalent protein–drug adduct ultimately provides conclusive evidence on the covalent binding mode. In ***Chapter 2***, we reviewed experimental technologies that can strictly distinguish a noncovalent protein–drug complex from a covalent protein–drug adduct, illustrated by examples from (recent) covalent drug development.[2] The experimental validation of covalent adduct formation is based on a detectable change that only occurs upon adduct formation:

an increased mass in the adduct (MS), continuous electron-density between protein and drug (protein crystallography), a change in intrinsic spectroscopic properties, chemical shift perturbation in covalently-bound inhibitor (NMR), fluorescence detection of proteins modified with inhibitor-derived ABPs (gel-based/homogeneous ABPP), or enrichment of ABP-modified proteins (chemoproteomic ABPP). Each technology has pros and cons: from compatibility with a reversible covalent binding mode or quantification of covalent occupancy, to mandatory chemical synthesis of labeled drug or incompatibility with complex mixtures. Aside from compatibility, another important factor is the informativeness of the technique: ranging from simple biophysical detection of the covalent adduct to detailed information on the modified amino acid residue, bond layout, and binding mode reversibility. Various MS techniques, protein crystallography, gel-based ABPP, and chemoproteomic ABPP platforms have been used to detect covalent protein–alkyne adducts in ***Chapter 4-6***.

In ***Chapter 3***, we expanded on the notion that evaluation of covalent binders uses different kinetic parameters to rank inhibitor potency (e.g. k_{inact}/K_I for irreversible covalent inhibitors), focusing on the connection between experimental assay conditions and algebraic models to obtain those kinetic parameters.[5] Most covalent inhibitors have a two-step binding mode – exerting their inhibitory effect through initial protein association forming a noncovalent complex, followed by covalent adduct formation that may or may not be reversible. Enzymatic assays to evaluate covalent inhibition capitalize on the time-dependence of covalent inhibition: a covalent adduct is not formed instantly (on a kinetic assay timescale) and inhibition improves with longer (pre)incubation times. The kinetic time-dependent enzyme activity can be fitted to algebraic models to extract relevant kinetic parameters. However, embedded in these algebraic equations are assumptions on experimental assay conditions – often implied but rarely explicitly mentioned – and is not always clear what the consequences are if those assumptions are violated. To understand kinetics and the impact of assay conditions, we composed kinetic simulation scripts that translate the mathematical equations into data read-out under relevant experimental assay conditions, which led to the identification of the general assumptions on experimental assay conditions. These simulations were then used to compose a comprehensive guide for evaluation of covalent inhibitors in enzymatic assays: four stepwise experimental protocols with accompanying data analysis protocols tailored to the covalent inhibitor binding mode.[5] A remaining challenge in the covalent drug development is the direct comparison of potency for reversible and irreversible inhibitors, as there is no shared/universal constant among these compound classes that facilitates hit prioritization. This may have complicated preclinical development, but other properties – such as metabolic stability, selectivity, ADME properties, hapten formation – are still deciding factors in the selection of suitable clinical candidates.

Part 2: Nonactivated Alkynes in Small Molecule Inhibitors

In ***Chapter 4***, we showed that a small recognition element (<600 Da) is compatible with the *in situ* thiol–alkyne reaction. Alkyne analogues of **odanacatib** (ODN, MK-0822) – a reversible covalent inhibitor of the main cysteine protease in bone resorption cathepsin K (CatK) – were obtained by replacing the nitrile warhead with an isoelectric alkyne moiety (**Figure 1**).[6]

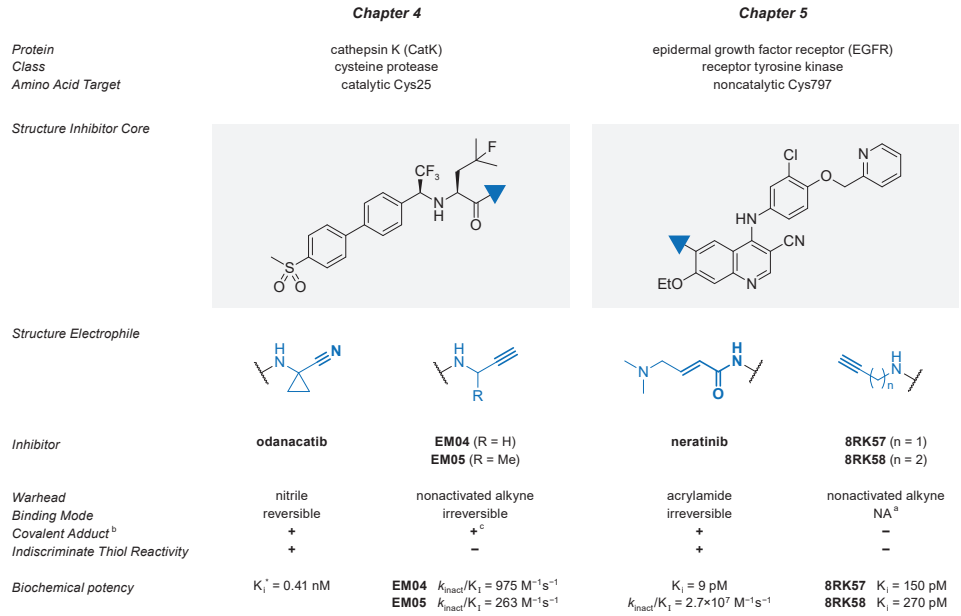

Figure 1 | The nonactivated alkyne warhead is compatible with covalent small molecule inhibition. Covalent alkyne derivatives of CatK inhibitor ODN (***Chapter 4***) and noncovalent alkyne derivatives of EGFR/HER2 inhibitor neratinib (***Chapter 5***). [a] Binding mode appears irreversible in cellular autophosphorylation assays but could not be confirmed in biochemical assays. [b] Detection of covalent protein–inhibitor adduct by intact protein MS. [c] Detection of covalent protein–inhibitor adduct by intact protein MS, bottom-up MS/MS, and protein crystallography. NA = not available.

Initially, *in vitro* activity assays showed that propargyl derivative EM04 had a >500-fold higher IC_{50} for hCatK inhibition than parent inhibitor ODN, comparable to the loss of potency in CatS inhibitor Leupeptin-**Prg** observed by Ekkebus *et al.*[3] However, further biochemical evaluation showed that nonactivated alkyne analogues have an irreversible covalent binding mode with hCatK, without undesired modification of nontargeted nucleophiles (e.g. GSH, Cys). Protein crystallography of the covalent adduct with desfluoro derivative EM07 (PDB: 6QBS) confirmed formation of a Markovnikov-type thiovinyl bond between the EM07 alkyne and the catalytic Cys25 of hCatK. The nonactivated alkyne derivatives have a surprisingly slow rate of covalent CatK–alkyne adduct formation, which may explain the apparent loss of potency in standard activity assays despite their irreversible binding mode: k_{inact} = 0.00019 s^{-1} and K_I^{app} = 211 nM for EM04. Indeed, the potency towards recombinant hCatK did not directly translate to inhibition of bone resorption activity in human osteoclast cultures: ODN was only 5-fold more potent than EM04. Interestingly, Western blotting for hCatK and visualization of active CatK with competitive irreversible qABP BMV109 showed that the level of mature CatK increased in inhibitor-treated osteoclasts, and BMV109 was able to outcompete the reversible binding of ODN. This may provide an explanation to the observed rebound effect in CatK activity in

mice/patients treated with ODN (discussed in more detail in *section 2.1*). Together, this work functions as a proof-of-concept that demonstrates how the nonactivated alkyne optimally balances on-target reactivity with excellent target selectivity, and can act as a latent electrophile in irreversible covalent small molecule inhibitors targeting a catalytic cysteine residue.

Having established that nonactivated alkynes can covalently target the catalytic cysteine residue of CatK, we investigated the possibility to target noncatalytic cysteines in ***Chapter 5***. To this end, the acrylamide warhead in approved covalent kinase inhibitor **neratinib** (Nerlynx, HKI-272) targeting noncatalytic Cys797 at the ATP-binding site of EGFR was replaced by propargylamine in 8RK57 or 1-amino-3-butyne in 8RK58 (**Figure 1**). A covalent adduct was not detected with GSH but also not with recombinant EGFR kinase domain. Preliminary cellular assays were indicative of an irreversible mode of action but kinase activity assays on recombinant EGFR kinase domain did not support this binding mode. It is unlikely that alkyne analogues 8RK57 and 8RK58 have a covalent binding mode, which may be attributed to inhibitor design (incorrect orientation of the alkyne relative to the cysteine thiol mitigating covalent adduct formation) or incompatibility of the thiol–alkyne reaction with noncatalytic cysteines (discussed in more detail in *section 2.4*). Altogether, covalent EGFR–alkyne adduct was not detected, but this does not definitively proof that the alkyne is incompatible with noncatalytic cysteine thiols. Alkyne derivatives of other kinase inhibitors may be required to further investigate the potential of the nonactivated alkyne warhead.

Part 3: Substituted Alkynes as Warheads in Ub-ABPs Targeting CysDUBs

Ekkebus *et al.*[3] found that Ub-ABPs with methylated internal alkyne Ub-**2** and *gem*-dimethylated propargylamide Ub-**5** did not form a covalent adduct with the recombinant purified CysDUB UCHL3, which led to the assumption that adduct formation is restricted to unsubstituted propargylamide. In ***Chapter 6***, we prepared a panel of propargylamine derivatives and incorporated them into fluorescent Rho-Ub-ABPs to investigate the role of various substituents.[7] Propargylamide analogues with substituents on the terminal or internal alkyne position were indeed unreactive toward recombinant UCHL3 but proceeded to form covalent adducts with other CysDUBs in whole cell lysates and recombinant protease. The acceptable position and bulkiness of substituents on the propargylamide was specific for the protease: selectivity was not conserved among members of the same CysDUB family. UCHL3 – the recombinant CysDUB that was selected for initial discovery – had a more restricted selectivity profile while USP16 is among the most flexible CysDUBs. Introduction of (bulky and/or electron-donating) methyl groups onto the propargylamide warhead reduces the rate of adduct formation with USP16 through steric as well as electronic effects. Mechanistically, adduct formation with Rho-Ub-**5** cannot proceed *via* an allenic intermediate (*mechanism C* in **Figure 5C**) – deprotonation of a *gem*-dimethylated propargylamide to form a reactive allenimide is not possible – but this may have been a USP16-specific exception to the general mechanism. The deuterated covalent adduct of recombinant USP16 and UCHL3 with deuterated propargylamide in Rho-Ub-[$\mathbf{D_2}$]-**Prg** confirmed that an alkyne rather than an allenic intermediate is the reactive species in the *in situ* thiol–alkyne reaction. Electron-deficient propargylamide ABP Rho-Ub-**18** bearing a trifluoromethyl group on the terminal position showed reactivity with noncatalytic cysteines

and was therefore not suited to study the mechanism of the thiol–alkyne reaction: adduct formation with electron-deficient alkynes can progress through an alternative, nonenzymatic mechanism with internal stabilization of a carbanion. Together, this work showed that the scope of the thiol–alkyne reaction is broader than initially assumed, and revealed an important role for the cysteine protease in the compatibility with bulky and/or electron-donating substituents on the propargylamide warhead.

2. Nonactivated Alkynes in Drug Development and Chemical Tools

Since its discovery one decade ago, the covalent thiol–alkyne reaction has gained a lot of traction. In the next sections, we will discuss the future prospects of irreversible CatK inhibition (*section 2.1*), the implementation of nonactivated alkynes in covalent small molecule inhibitors (*section 2.2*), the role of (substituted) propargyl warheads in Ub(l)-ABPs (*section 2.3*), and give an overview of the possible mechanisms of the thiol–alkyne reaction (*section 2.4*).

2.1. Covalent Alkynes in Irreversible CatK Inhibitor Development

Odanacatib (ODN) was the fourth CatK inhibitor that failed in clinical phase II or III, after more than twelve years in clinical development, and pharmaceutical companies seem to have abandoned CatK inhibitors as osteoporosis treatment agents considering the long list of failed attempts.[8-11] Osteoporosis a systemic skeletal condition that affects the elderly population: half of the (postmenopausal) women are likely to experience at least one osteoporotic fracture in their lifetime.[12] The disease is characterized by an unbalance in bone formation and degradation, resulting in fragile and brittle bones that are susceptible to fractures induced by mild stress such as falling or coughing.[13] Among the treatment options are bisphosphonates: anti-resorptive agents that have a direct apoptotic effect on osteoclasts but can also inhibit activity and proliferation of bone-forming osteoblasts. These agents suppress bone formation along with inhibition of bone degradation, and treatment benefits typically plateau after only three years.[10] ODN was supposed to be Merck's next big blockbuster drug for long-term osteoporosis treatment because of its once-weekly oral administration without concurrent bone formation suppression. Unfortunately, ODN development was discontinued in 2016 due to an increased risk of stroke, atrial fibrillation, cerebrovascular events and overall death.[9, 14] These adverse effects were unexpected as they are not common in pycnodysostosis [15] – a rare autosomal recessive lysosomal storage disorder associated with production of inactive CatK due to a *CTSK* gene mutation – and preclinical *in vitro* studies mostly indicate that CatK inhibition has a cardioprotective effect.[8, 16-17] Although it is known that the effect of *CTSK* mutations or knock-down differs from (long-term) CatK inhibition, [18] it is surprising to observe the opposite effect.

2.1.1. Adverse Effects/Rebound Effect

The exact underlying mechanism to the adverse effects is unknown at this moment, but it is possible that these are on-target adverse effects related to CatK functions that are not related to bone resorption.[16, 19] CatK inhibition causes structural ECM remodeling, and it has been

postulated that this increases the risk of atrial arrhythmia.[14] Ischemic stroke is typically caused by blockage of an artery supplying blood to the brain. This blockage can be a blood clot consisting of an intact plaque or a ruptured plaque.[20] Plaque stability decreases upon overexpression of CatK,[21] or may be the result of the rebound effect resulting in high levels of active mature CatK. A rebound effect has been reported *in vitro* but also in patients: bone resorption activity and osteoclast numbers are elevated during and after ODN treatment.[8, 22-23] In line these observations, we observed an elevated level of mature CatK in human osteoclasts upon treatment with CatK inhibitors (***Chapter 4***).[6] We also found that irreversible qABP BMV109 was able to outcompete ODN, resulting in regained CatK activity that exceeded the activity in vehicle-treated samples. Furthermore, treatment discontinuation studies *(unpublished data)* revealed increased bone resorption activity after discontinuation of ODN treatment (**Figure 2**). This rebound effect was not observed in samples treated with our irreversible CatK inhibitor EM04: catalytic activity of irreversibly inhibited mature CatK cannot be regained. Therefore, we believe that the adverse effects of ODN may be related to the rebound effect that is specific for reversible CatK inhibition, which can be avoided by irreversible CatK inhibitors.

To establish whether the adverse effects are resultant from a rebound effect associated with reversible CatK inhibition, further research is needed. This would include elucidation of the feedback mechanisms that drive osteoclast maturation and CatK expression, identification of proteases involved in mature CatK degradation, and evaluation how (ir)reversible inhibition affects CatK activity and expression levels in non-skeletal tissue. Finally, (expensive) long-term clinical trials are needed to validate whether irreversible CatK inhibition does indeed reduce rebound and possible on-target adverse effects.

2.1.2. CatK Inhibitors for Treatment of Metastatic Bone Disease

Aberrant bone resorption is not only associated with osteoporosis but also with other (skeletal) conditions including Paget's disease of bone,[24] periodontal disease,[25] rheumatoid arthritis,[26] osteoarthritis,[27] periprosthetic osteolysis,[28] osteolytic bone disease,[29] metastatic bone disease,[30] and giant cell tumor of the bone.[31] In metastatic bone disease with an osteolytic phenotype, tumors originating from other tissues metastasize to the bone where they enhance differentiation and activation of osteoclasts, ultimately leading to degradation of the bone matrix.[32-33] Treatment options are overlapping with treatment options for osteoporosis:[34] osteoclast inhibitors suppress bone resorption, thereby reducing bone pain, decreasing the incidence of skeletal-related events, and preventing the formation of new osteolytic lesions.[35-36] The bisphosphonate antiresorptive agents target the osteoclasts recruited by the metastasized tumor, but do not inhibit CatK secreted by the tumor itself: giant cell tumors of the bone and (invasive subpopulations of) tumors that metastasized to the bone have been reported to (over)express hCatK.[15, 31, 37-40] Selective CatK inhibition has been reported to reduce cancer cell invasiveness, thereby possibly preventing the formation of (bone) metastases.[15, 37-38] The benefit:risk ratio for CatK inhibition is more likely to be positive for these patient populations as they are expected to have a shorter treatment period (and life expectancy) relative to long-term treatment of osteoporosis patients. Younger patients may also be less prone to some adverse effects – post-menopausal and osteoporotic women have an increased stroke risk [41-42] and have more unstable plaques.[43]

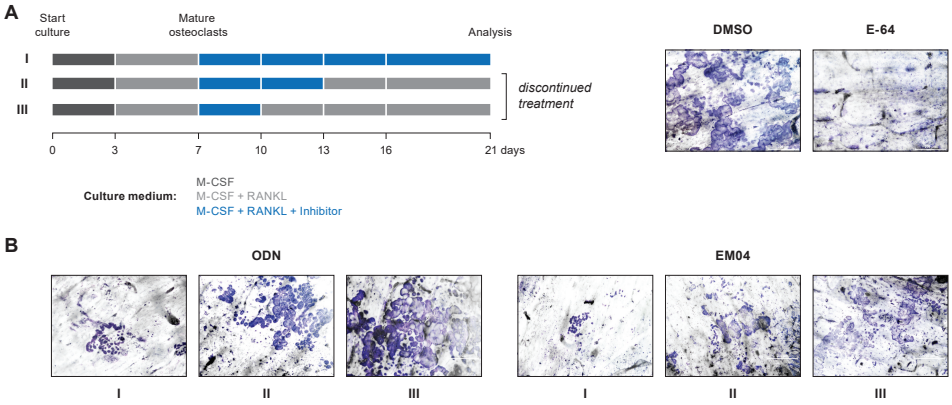

Figure 2 | Preliminary data on CatK activity in human osteoclasts (OCs), upon discontinuation of inhibitor treatment. **(A)** Discontinuation (washout) experiment. Adjustment of the protocol used in ***Chapter 4***. Culture medium containing either inhibitor or DMSO was refreshed on day 7, 10, 13, and 16. In *conditions II* and *III*, inhibitor treatment was discontinued by washout and refreshing with medium that does not contain inhibitor. On day 21, OCs were washed away and lysed, and bone slices were stained with Coomassie Brilliant Blue to visualize bone resorption. **(B)** Bone resorption in cultures treated with 2 µM ODN or EM04. Normal (trench-forming) bone resorption activity is regained after approximately 7 days *(II)*. Discontinuation of ODN results in elevated levels of bone resorption relative to the DMSO control *(III)*.

Preclinical studies indicate that selective CatK inhibitors prevent establishment and progression of bone metastases of various solid cancers,[44-47] and a phase II clinical study of ODN in breast cancer patients with established bone metastases confirmed target engagement.[48] Unfortunately, we were unable to investigate the *in vivo* efficacy of EM04, because murine CatK (mCatK) – despite sharing 88% homology with human (hCatK) – contains mutations at the enzyme active site that hinder formation of a covalent adduct with active site-directed inhibitors such as ODN.[49] Established murine disease models to study bone metastases can use human tumor material, but the native osteoclasts still express mCatK, rendering them unsuited as model system.[50] Rabbits (94% homology) and monkeys (identical to hCatK) are more suitable to study the effects of irreversible covalent CatK inhibition.[8] However, a transgenic mouse model with a humanized *CTSK* expressing hCatK or mCatK^{Y61D} – that can be covalently modified by active site-directing inhibitors – would be desirable as they could be employed in established murine models of skeletal disease. To our knowledge, humanized murine models with CatK chimeras have not yet been developed.

2.2. Nonactivated Alkynes in Recent Covalent Drug Development

In ***Chapter 4***, our irreversible covalent alkyne derivatives of CatK inhibitor **odanacatib** (ODN, MK-0822) demonstrated that the nonactivated propargyl warhead can act as a latent electrophile in covalent small molecule inhibitors (<600 Da) targeting a catalytic cysteine.[6] We also found that covalent CatK–alkyne adduct formation is relatively slow, which was an

unexpected finding considering that CysDUB–Ub-**Prg** adduct formation is quantitative within minutes (***Chapter 6***).[7] The covalent binding mode would have been overlooked without direct detection of the covalent adduct (***Chapter 2***)[2] and kinetic evaluation (***Chapter 3***),[5] underlining the crucial importance of dedicated methods tailored to (ir)reversible inhibition. Our proof-of-concept with CatK demonstrated that a small recognition element can be sufficient for covalent thiovinyl adduct formation, and nonactivated terminal alkynes have since gained popularity as irreversible covalent warheads. Our approach of replacing a nitrile warhead for an isoelectric alkyne warhead has since been employed to other cysteine protease targets (**Figure 1**, **Figure 3**).

Behring *et al.*[51] report an extensive panel of dipeptide-derived alkynes and nitriles specifically targeting cathepsin B, S, K or L (**Figure 3**). The covalent binding mode was deduced from irreversibility in a 5-fold dilution assay and kinetic behavior instead of biophysical detection of the covalent protein–inhibitor adduct. Interestingly, reversible binding potency of a dipeptide nitrile did not necessarily translate to a potent alkyne derivative, underlining that alkyne-based covalent drugs would benefit from optimization of noncovalent interactions. These potentially covalent cathepsin dipeptide alkynes are fascinating when we consider that, in the original work by Ekkebus *et al.*[3] covalency was not observed with alkyne derivatives of CatS inhibitor Leupeptin (a tripeptide-aldehyde) or Casp1 inhibitor Ac-YVAD-**CHO** (a tetrapeptide-aldehyde). It is possible that Leupeptin-**Prg** – replacing the reversible covalent aldehyde warhead with a propargyl derivative – may actually have had a covalent binding mode: Leupeptin-**Prg** was assumed to have a noncovalent binding mode because of its dramatic loss of potency in enzymatic activity assays, similar to what we observed for alkyne derivative EM04, which is in agreement with slow covalent thiovinyl bond formation. Tetrapeptide Ac-YVAD-**Prg** (488 Da) was also assumed to be a noncovalent inhibitor of cysteine protease caspase-1 (Casp1) due to its low inhibitory potency in enzymatic assays – detecting the combined noncovalent and covalent inhibition after a short preincubation – while covalent adduct of Casp1 with Cy5-IL-1$\beta_{102-116}$-**Prg** peptide (having a recognition element of 1.8 kDa, excluding the Cy5 fluorophore) was successfully detected by in-gel fluorescence – strictly detecting covalent adducts. Together, this led to the incorrect assumption that the covalent thiol–alkyne reaction requires a relatively large recognition element, as we demonstrated with our covalent alkyne-based small molecule CatK inhibitors.[6]

Brewitz *et al.*[52] prepared various terminal/internal alkyne derivatives of COVID-19 drug **nirmatrelvir** (Paxlovid, PF-07321332) and several other inhibitors of SARS-CoV-2 main protease (M^{pro}), and made a side-by-side comparison of the IC_{50} of parent nitriles and their alkyne derivatives (**Figure 3**). Nirmatrelvir alkyne derivative **13** was initially found to be less potent than the parent nitrile, but alkyne derivatives generally retain their activity against the S144A mutant M^{pro} better than the nitriles. Ser144 is part of the oxyanion hole thus helping to stabilize a tetrahedral anionic intermediate, and Ser144 variations reduce nirmatrelvir potency, which may enable development of nirmatrelvir resistance. Protein crystallography provided mechanistic rational to this observation: the thioimidate nitrogen in the covalent M^{pro}–nirmatrelvir adduct is positioned in the oxyanion hole (PDB: 7TE0) whereas the terminal olefin carbon in the covalent M^{pro}–alkyne adduct is pointing away from these residues

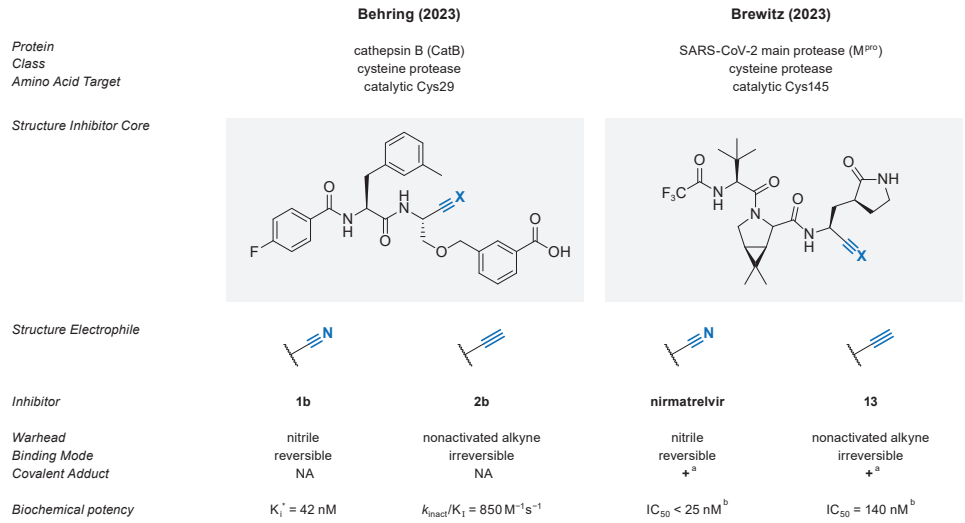

Figure 3 | Nonactivated alkynes as covalent warheads targeting the catalytic cysteine residue in small molecule inhibitors. Irreversible alkyne analogues were obtained by replacing the nitrile warhead by an isoelectric (substituted) propargyl warhead. Behring *et al.*[51] developed cathepsin B (CatB) inhibitors with a dipeptide recognition element. Brewitz *et al.*[52] replaced the nitrile warhead of SARS-CoV-2 M^{pro} inhibitor nirmatrelvir (Paxlovid, PF-07321332) with an alkyne warhead. [a] Detection of covalent protein–inhibitor adduct by intact protein MS and protein crystallography. [b] Biochemical IC_{50} after preincubation of 50 nM enzyme with inhibitor for 15 min.

(PDB: 8B2T). This observation suggests that an anionic thioimidate intermediate is stabilized in the oxyanion hole, whereas covalent thiol–alkyne addition does not involve a carbanion intermediate or is quickly protonated.

Ngo *et al*. synthesized the same nirmatrelvir derivative with a nonactivated alkyne (**4d**), and a two-step ABP derivative **Alk-4d**.[53] Furthermore, they then used a two-step ABP **Alk-4i** bearing an electron-deficient trifluoromethylated alkyne as warhead and terminal alkyne as a Click handle to study the residence time of nirmatrelvir, as this modification increased the reactivity (and reaction rate), stating the faster reactivity with this 'latent' electrophile is beneficial for SARS-CoV-2 inhibition. In agreement with our findings in ***Chapter 6***,[7] they do observe non-specific proteome labeling with **Alk-4i**, so it is debatable if the trifluoromethylated alkyne actually is a latent electrophile.

Together with the work in this dissertation, the recent incorporation of alkynes into other protease inhibitors underscore the role nonactivated alkynes may have as latent electrophiles in small molecule covalent drug development. Nonactivated alkynes are now not only incorporated by late-stage replacement of a covalent nitrile, but have also been included in a panel of established covalent warheads for the rational design of novel SARS-CoV-2 M^{pro} inhibitors [54-55] and covalent TKIs targeting Cys552 in FGFR4.[56] It is unlikely that covalent alkynes

will be identified in covalent fragment screening – covalent fragments (<200 Da) are unlikely to position the alkyne in sufficient proximity to a reactive cysteine thiol to initiate covalent adduct formation – nor do we expect that these findings will affect the use of acetylenes as bioorthogonal handles, but we imagine a promising role for the alkyne warhead in rational/structure-based covalent drug design.

2.3. The Propargylamide Warhead in Ub(l)-ABPs

Since its discovery in 2013, the propargyl (**Prg** or **PA**) warhead has been incorporated into numerous other Ubl-based ABPs including Rho-UFM1-**Prg**,[57] ISG15-**Prg**,[58] and LC3-**Prg**,[59] into ubiquitin variant (UbV) ABPs with specificity for USP7,[60] USP16,[61] or UCHL3,[62] and into nonhydrolyzable diUb-**Prg** ABPs with a propargylamide warhead on the proximal C-terminus that bind to the protease S1-S2 sites.[63] Nowadays, the covalent **Prg** warhead is considered the golden standard for cysteine-reactive Ub(l)-ABPs: the high stability in physiological conditions and absence of intrinsic reactivity with nontargeted thiols and noncatalytic cysteines is superior to any other (acid-stable) warhead.[64-65] Furthermore, Ub(l)-**Prg** ABPs are readily obtained by SPPS in high purity and, contrary to Ub-**VME**, the **Prg** warhead can be installed using cheap and commercially available propargylamine. The superior selectivity for catalytic cysteines is an important feature of Ub(l)-**Prg**: labeling of noncatalytic cysteines in HEK293T lysate has not been found with HA-Ub-**Prg** but was identified for HA-Ub-**VME** and HA-Ub-**VS**.[64] These findings were supported in ***Chapter 6***, where minor adduct formation was detected for Rho-Ub-**VME** and Rho-Ub-**18** with catalytically inactive USP16^{C205A} mutant but not for Rho-Ub-**Prg**. Another compelling reason to use Ub-**Prg** ABPs in chemoproteomic profiling is the improved reactivity that some CysDUB classes have toward **Prg** compared to **VME** or **Br2**, which enabled comprehensive coverage of the DUBome with HA-Ub-**Prg**.[65] Ub(l)-**Prg** ABPs were also instrumental in crystallographic studies to solve the Ub(l)-bound structures of cysteine proteases as well as the HECT domain of various E3 ligases.[66-67]

In ***Chapter 6***, we incorporated substituted propargylamine derivatives into Ub-ABPs and discovered that compatibility with electron-donating/bulky substituents is driven by the individual CysDUBs. These substituted propargylamide warheads can be used in the design of CysDUB-selective Ub-ABPs, and our panel of propargylamine derivatives can also conveniently be incorporated into other Ubl-ABPs (e.g. SUMO2-**Prg**, ISG15-**Prg**) to investigate the selectivity (and inhibition) of the corresponding Ubl proteases. We also showed how Rho-Ub-ABPs can be used in quantitative FP binding assays and quantitative gel analysis to evaluate ABP potency in a noncompetitive manner. There is a clear need for quantitative assays to evaluate inhibitor potency, and we have identified several ligand binding competition assay methodologies where Ub-ABPs can act as (ir)reversible ligands. These methodologies are compatible with gel-based or MS-based detection of the enzyme–ABP adduct (***Chapter 2***). For application in high-throughput and/or homogeneous assays – without removal of unbound ABP – Ub-based qABPs or turn-on ABPs would be more suitable.[68] For example, we predict that ABPs such as Ub-**Prg** can be used to evaluate irreversible cysteine-targeting inhibitors in a preincubation assay using the same concept as *Method IV* in ***Chapter 3***. This ligand binding competition assay is theoretically compatible with CysDUBs, and this concept might also be applicable to more

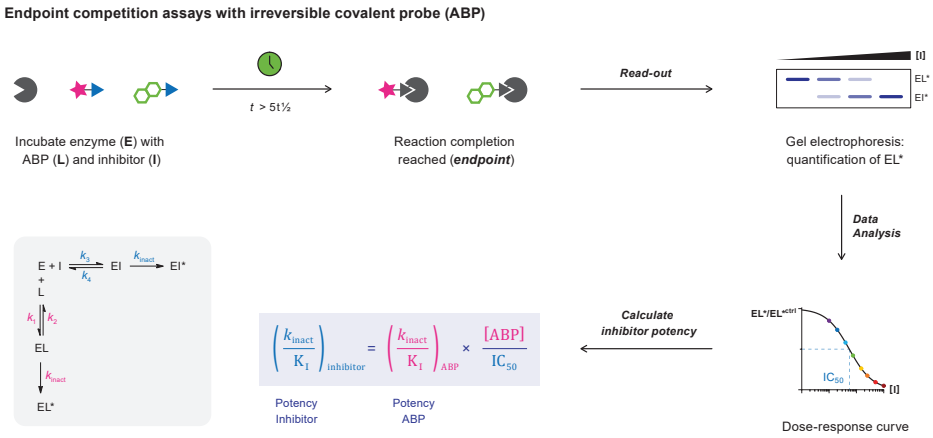

Figure 4 | Endpoint competition assay with irreversible covalent ABPs by Miyahisa *et al.*[69] Enzyme (E) is incubated with inhibitor (I) and irreversible ABP (L) until reaction completion/endpoint (t > 5t½): full covalent occupancy of enzyme by inhibitor (EI*) or ABP (EL*). Quantification of covalent enzyme–ABP adduct (EL*) at different inhibitor concentrations enables calculation of an IC_{50}. The inhibitor k_{inact}/K_I is then calculated using the IC_{50}, ABP concentration and ABP k_{inact}/K_I, thus only requiring in-depth kinetic evaluation of the ABP. Read-out before reaction completion is reached (t < 5t½) results in overestimation of inhibitor k_{inact}/K_I because enzyme–ABP adduct formation is not yet complete.

challenging targets such as E2/E3 ligases, as long as the enzyme has a catalytic cysteine residue. We also foresee that Ub-ABPs may also be used in an endpoint competition assay methodology developed at Takeda (**Figure 4**).[69] Using a well-characterized irreversible covalent ABP, irreversible covalent inhibitor potency (k_{inact}/K_I) can be determined from the dose-response of covalent ABP occupancy, without needing to perform detailed kinetic measurements for each inhibitor. This method has the best accuracy when the potency of ABP and inhibitor is within a few orders of magnitude: the inhibitor will not be able to form a covalent enzyme–inhibitor adduct if the ABP is too potent (and fully occupies the enzyme in the enzyme–ABP adduct). The relatively slow adduct formation of Ub-**Prg** with the catalytic cysteine of E2/E3 ligases may be compatible with this method, though we expect Ub-**Prg** to be too potent to use with CysDUBs. We foresee a role for our Ub-ABPs with a substituted propargylamide warhead that have a slower reaction rate (e.g. Ub-**2**).

2.4. Mechanism of Thiol–Alkyne Addition

One of the central unanswered questions in 2013 was by which mechanism the thiol–alkyne addition proceeds (**Figure 5**). In ***Chapter 6***, we detected the covalent adduct of USP16 with gem-dimethylated propargyl analogue Rho-Ub-**5**, which could not have occurred *via* an allenic intermediate. Subsequent bottom-up MS detection of adducts with deuterated ABP Ub-[$\mathbf{D_2}$]-**Prg** provided conclusive evidence that the thiol–alkyne reaction does not involve an allenic intermediate, thereby excluding *mechanism C* (**Figure 5C**).[7]

Radical-mediated *mechanism A1* had already been excluded because thiol–yne coupling (TYC) generates the incorrect *anti*-Markovnikov-type adduct (**Figure 5A**). There is no conclusive evidence to exclude radical-initiated *mechanism A2*, but Markovnikov hydrothiolation of ynamides typically occurs *via* an allenic intermediate,[70-71] which was excluded in ***Chapter 6***. The reactions with Ub-**Prg** in our work were performed in strict absence of light – thiyl radicals degrading pharmaceutical products are primarily formed upon exposure to light[72-73] – but it should be noted that cysteinyl radicals have a role in redox regulation of enzyme activity, also in absence of light, as is utilized by specific enzyme classes (e.g. radical *S*-adenosylmethionine (SAM) enzymes, glycyl radical enzymes, and ribonucleotide reductases).[74] A more compelling argument is the observed lack of spontaneous CysDUB reactivity with Ub probes bearing an allyl warhead reported by Taylor *et al*.[75] The radical-initiated thiol–ene reaction to form a covalent CysDUB–ABP adduct had to be promoted by a radical initiator combined with UV irradiation: a higher intrinsic reactivity with the allyl warhead can be expected if spontaneous thiyl radical formation at the CysDUB cysteine was a common occurrence.

The remaining mechanisms for the thiol–alkyne addition are direct nucleophilic attack with concerted protonation (*mechanism B* in **Figure 5B**) or a stepwise mechanism with stabilization of the carbanion intermediate in the protease oxyanion hole (*mechanism D* in **Figure 5D**). Adduct formation has been detected with cysteine proteases (e.g. CysDUBs, cathepsins, M^{pro}), which have a nucleophilic cysteine residue essential for proteolytic function that is part of a catalytic triad/dyad, and an oxyanion hole to stabilize an anionic (tetrahedral) intermediate,[76] which may indicate a role for the oxyanion hole in the thiol–alkyne addition (*mechanism D*). However, this is contradicted by the adduct formation with SENP1^{Q597A} mutant.[4] An alternative explanation is that catalytic cysteines are simply more nucleophilic – and are typically deprotonated by neighboring basic residues generating the reactive thiolate anion – thus driving the observed reactivity. Unfortunately, CysDUB adduct formation with Rho-Ub-**18** bearing electron-deficient alkyne **18** (terminal CF_3) in ***Chapter 6*** does not provide evidence on the mechanism of the thiol–alkyne reaction: electron-deficient alkynes have the ability to internally stabilize an anionic intermediate, and may have a different reaction mechanism than nonactivated alkynes. This is confirmed by the higher intrinsic thiol reactivity with nontargeted thiols such as GSH.

The reaction mechanism impacts the possible application to other protein classes: if the selectivity for cysteine proteases over nontargeted thiols is due to stabilization of a carbanion intermediate in an oxyanion hole, then this would restrict adduct formation to (catalytic) cysteines in enzymes bearing an oxyanion hole. By itself, such selectivity is favored but it will restrict applications to catalytic protease cysteines as it will not be compatible with noncatalytic cysteine residues in other protein classes. Covalent adducts with alkyne derivatives 8RK57 and 8RK58 – based on approved covalent dual EGFR/HER2 inhibitor **neratinib** (Nerlynx, HKI-272) – were not observed in ***Chapter 5***, suggestive of a role for the oxyanion hole. However, our alkyne derivatives not having a covalent binding mode does not rule out *mechanism B* as this might have been an inhibitor-specific issue: identification of a single covalent kinase inhibitor with an nonactivated alkyne warhead would still provide conclusive evidence that the thiol–alkyne adduct formation does not involve stabilization in an oxyanion hole. Importantly,

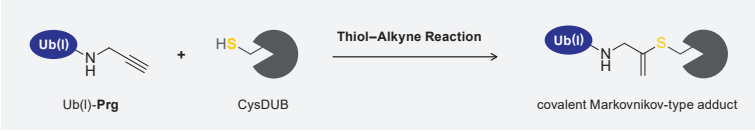

A Radical Thiyl Addition to Alkyne

Mechanism A1
+ Established Thiol–Yne Coupling (TYC) mechanism
− Anti-Markovnikov product is incorrect

Mechanism A2
+ Unexpected mechanism for unexpected reaction
− Unfavored radical addition to hindered carbon
− Low reactivity with allyl in radical thiol–ene reaction

B Concented Nucleophilic Thiolate Addition to Alkyne

Mechanism B
+ Adduct with SENP1^{Q597A} mutant
+ Olefin carbon away from oxyanion hole in crystal
+ Computational model indicative of concerted
− Inactive with noncatalytic cysteine in EGFR

C Nucleophilic Thiolate or Radical Thiyl Addition to Allenic Intermediate

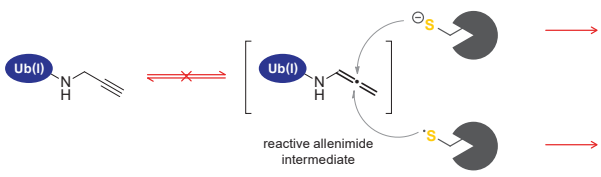

Mechanism C1
+ Allenimides are established electrophiles
− Reactivity at high pH
− Adduct with Ub-**5** and Ub-**[D_2]-Prg**

Mechanism C2
+ Radical addition to hindered carbon
− Reactivity at high pH
− Adduct with Ub-**5** and Ub-**[D_2]-Prg**

D Stepwise Nucleophilic Thiolate Addition to Alkyne

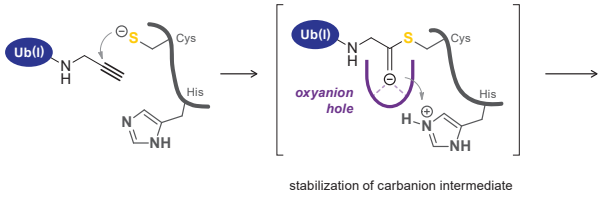

Mechanism D
+ Resembles proteolysis mechanism
+ Adduct formation restricted to catalytic cysteines
− Reactivity with SENP1^{Q597A} mutant
− Olefin carbon away from oxyanion hole in crystal

Figure 5 | Reaction mechanisms for Markovnikov-type thiovinyl adduct formation between a catalytic cysteine thiol(ate) and an alkyne warhead, and reasons supporting (+) or contradicting (–) this mechanism. **(A)** Direct addition of thiyl radical to the terminal alkyne is unlikely. **(B)** Proximity-driven *in situ* thiol–alkyne addition with concerted nucleophilic attack and protonation is a possible mechanism. **(C)** Tautomerization of the terminal alkyne moiety to a thiol-reactive allenimide intermediate at the enzyme active site prior to nucleophilic *(top)* or radical *(bottom)* addition has been excluded. **(D)** Stepwise enzyme-templated thiol(ate)–alkyne addition *via* stabilization of a secondary carbanion intermediate in the enzyme oxyanion hole is a possible mechanism.

a concerted reaction *(mechanism B)* does not necessarily mean that the *in situ* thiol–alkyne addition is compatible with noncatalytic cysteines: a histidine or another basic moiety in the vicinity of the cysteine may be required for concerted protonation, although adduct formation of SUMO2-**Prg** with SENP1^{H533A} suggests otherwise (***Chapter 1***).[4]

In *section 2.2* we already noticed that the terminal olefin carbon in crystal structures of covalently bound alkynes was pointing away from residues in the oxyanion hole,[52] which is suggestive of concerted *mechanism B* (**Figure 5B**). MD-based analysis by Endres *et al.*[77] of the EM07–CatK structure suggests that the alkyne is positioned outside of the binding pocket. The likeliness of a concerted versus stepwise reaction mechanism has further been investigated by computational modelling. Dos Santos and co-workers employed (QM/MM) molecular dynamics reaction simulations to characterize the covalent reaction of CatK with nitrile ODN and alkyne derivatives EM04, EM05 and EM06 at an atomic level.[78] The crystal structure of the covalent CatK–EM07 adduct (PDB: 6QBS) was used as a starting point to build the computational models of the inhibitors in an enzymatic environment. Free-energy profiles of reaction with nitriles and alkynes showed that nucleophilic thiolate attack by catalytic Cys25 occurs in a concerted manner with proton transfer by the catalytic His162, supporting the *in situ* thiol–alkyne addition of *mechanism B*. The existence of an anionic intermediate could not be excluded for activated bromoalkyne EM06 but was deemed unlikely for ODN, EM04, and EM05. By comparison, (QM/MM) molecular dynamics reaction simulations of covalent adduct formation between ibrutinib and BTK Cys481 suggest a stepwise mechanism, initiated by direct proton transfer from Cys481 to the acrylamide warhead.[79] However, as with most computational models,[80-81] potentially stabilizing interactions with Gln19 and other residues in the CatK oxyanion hole were disregarded.[82] It is therefore not possible to definitively exclude *mechanism D* based on these computational results.

Altogether, the currently available data strongly indicates that nucleophilic attack on the alkyne, in a concerted or stepwise manner, is the most likely mechanism for the *in situ* thiol–alkyne reaction. Regardless of the mechanism, future efforts to unlock the full potential of the nonactivated alkyne as a latent electrophile in covalent drug development should focus on the development of nonactivated alkyne-based kinase inhibitors.

"And they lived happily ever after"

3. References

1. De Vita, E. 10 Years into the Resurgence of Covalent Drugs. *Future Med. Chem.* **2021**, *13*, 193-210. doi: 10.4155/fmc-2020-0236.
2. Mons, E.; Kim, R.Q.; Mulder, M.P.C. Technologies for Direct Detection of Covalent Protein–Drug Adducts. *Pharmaceuticals* **2023**, *16*, 547. doi: 10.3390/ph16040547.
3. Ekkebus, R.; van Kasteren, S.I.; Kulathu, Y.; Scholten, A.; Berlin, I.; Geurink, P.P.; de Jong, A.; Goerdayal, S.; Neefjes, J.; Heck, A.J.R.; Komander, D.; Ovaa, H. On Terminal Alkynes That Can React with Active-Site Cysteine Nucleophiles in Proteases. *J. Am. Chem. Soc.* **2013**, *135*, 2867-2870. doi: 10.1021/ja309802n.
4. Sommer, S.; Weikart, N.D.; Linne, U.; Mootz, H.D. Covalent Inhibition of SUMO and Ubiquitin-Specific Cysteine Proteases by an In Situ Thiol–Alkyne Addition. *Bioorg. Med. Chem.* **2013**, *21*, 2511-2517. doi: 10.1016/j.bmc.2013.02.039.
5. Mons, E.; Roet, S.; Kim, R.Q.; Mulder, M.P.C. A Comprehensive Guide for Assessing Covalent Inhibition in Enzymatic Assays Illustrated with Kinetic Simulations. *Curr. Protoc.* **2022**, *2*, e419. doi: 10.1002/cpz1.419.
6. Mons, E.; Jansen, I.D.C.; Loboda, J.; van Doodewaerd, B.R.; Hermans, J.; Verdoes, M.; van Boeckel, C.A.A.; van Veelen, P.A.; Turk, B.; Turk, D.; Ovaa, H. The Alkyne Moiety as a Latent Electrophile in Irreversible Covalent Small Molecule Inhibitors of Cathepsin K. *J. Am. Chem. Soc.* **2019**, *141*, 3507-3514. doi: 10.1021/jacs.8b11027.
7. Mons, E.; Kim, R.Q.; van Doodewaerd, B.R.; van Veelen, P.A.; Mulder, M.P.C.; Ovaa, H. Exploring the Versatility of the Covalent Thiol–Alkyne Reaction with Substituted Propargyl Warheads: A Deciding Role for the Cysteine Protease. *J. Am. Chem. Soc.* **2021**, *143*, 6423-6433. doi: 10.1021/jacs.0c10513.
8. Drake, M.T.; Clarke, B.L.; Oursler, M.J.; Khosla, S. Cathepsin K Inhibitors for Osteoporosis: Biology, Potential Clinical Utility, and Lessons Learned. *Endocr. Rev.* **2017**, *38*, 325-350. doi: 10.1210/er.2015-1114.
9. Mullard, A. Merck & Co. Drops Osteoporosis Drug Odanacatib. *Nat. Rev. Drug Discov.* **2016**, *15*, 669-669. doi: 10.1038/nrd.2016.207.
10. Garber, K. Two Pioneering Osteoporosis Drugs Finally Approach Approval. *Nat. Rev. Drug Discov.* **2016**, *15*, 445-446. doi: 10.1038/nrd.2016.132.
11. Lowe, D. Cathepsin K: A Promising Target Fades Out. *In the Pipeline* [Online], 2016, 30 September. https://www.science.org/content/blog-post/cathepsin-k-promising-target-fades-out.
12. Johnell, O.; Kanis, J. Epidemiology of Osteoporotic Fractures. *Osteoporos. Int.* **2005**, *16*, S3-S7. doi: 10.1007/s00198-004-1702-6.
13. U.S. Department of Health and Human Services. *Bone Health and Osteoporosis: A Report of the Surgeon General*. U.S. Department of Health and Human Services, Office of the Surgeon General: Rockville (MD), 2004. https://www.ncbi.nlm.nih.gov/books/NBK45513/.
14. McClung, M.R.; O'Donoghue, M.L.; Papapoulos, S.E.; Bone, H.; Langdahl, B.; Saag, K.G.; Reid, I.R.; Kiel, D.P.; Cavallari, I.; Bonaca, M.P., et al. Odanacatib for the Treatment of Postmenopausal Osteoporosis: Results of the LOFT Multicentre, Randomised, Double-Blind, Placebo-Controlled Trial and LOFT Extension Study. *Lancet Diabetes Endocrinol.* **2019**, *7*, 899-911. doi: 10.1016/S2213-8587(19)30346-8.
15. Verbovšek, U.; Van Noorden, C.J.F.; Lah, T.T. Complexity of Cancer Protease Biology: Cathepsin K Expression and Function in Cancer Progression. *Semin. Cancer Biol.* **2015**, *35*, 71-84. doi: 10.1016/j.semcancer.2015.08.010.
16. Dai, R.; Wu, Z.; Chu, H.Y.; Lu, J.; Lyu, A.; Liu, J.; Zhang, G. Cathepsin K: The Action In and Beyond Bone. Front. *Cell Dev. Biol.* **2020**, *8*, 433. doi: 10.3389/fcell.2020.00433.
17. Guo, R.; Hua, Y.; Rogers, O.; Brown, T.E.; Ren, J.; Nair, S. Cathepsin K Knockout Protects Against Cardiac Dysfunction in Diabetic Mice. *Sci. Rep.* **2017**, *7*, 8703. doi: 10.1038/s41598-017-09037-z.
18. Brömme, D.; Panwar, P.; Turan, S. Cathepsin K Osteoporosis Trials, Pycnodysostosis and Mouse Deficiency Models: Commonalities and Differences. *Expert Opin. Drug Discov.* **2016**, *11*, 457-472. doi: 10.1517/17460441.2016.1160884.
19. Mijanović, O.; Jakovleva, A.; Branković, A.; Zdravkova, K.; Pualic, M.; Belozerskaya, T.A.; Nikitkina, A.I.; Parodi, A.; Zamyatnin, A.A. Cathepsin K in Pathological Conditions and New Therapeutic and Diagnostic Perspectives. *Int. J. Mol. Sci.* **2022**, *23*, 13762. doi: 10.3390/ijms232213762.
20. Rothwell, P.M. Atherothrombosis and Ischaemic Stroke. *Br. Med. J.* **2007**, *334*, 379. doi: 10.1136/bmj.38964.489051.80.
21. Samokhin, A.O.; Wong, A.; Saftig, P.; Brömme, D. Role of Cathepsin K in Structural Changes in Brachiocephalic Artery During Progression of Atherosclerosis in apoE-Deficient Mice. *Atherosclerosis* **2008**, *200*, 58-68. doi: 10.1016/j.atherosclerosis.2007.12.047.
22. Leung, P.; Pickarski, M.; Zhuo, Y.; Masarachia, P.J.; Duong, L.T. The Effects of the Cathepsin K Inhibitor Odanacatib on Osteoclastic Bone Resorption and Vesicular Trafficking. *Bone* **2011**, *49*, 623-635. doi: 10.1016/j.bone.2011.06.014.
23. Recker, R.; Dempster, D.; Langdahl, B.; Giezek, H.; Clark, S.; Ellis, G.; de Villiers, T.; Valter, I.; Zerbini, C.A.F.; Cohn, D.; Santora, A.; Duong, L.T. Effects of Odanacatib on Bone Structure and Quality in Postmenopausal Women With Osteoporosis: 5-Year Data From the Phase 3 Long-Term Odanacatib Fracture Trial (LOFT) and Its Extension. *J. Bone Miner. Res.* **2020**, *35*, 1289-1299. doi: 10.1002/jbmr.3994.
24. Reddy, S.V. Etiology of Paget's Disease and Osteoclast Abnormalities. *J. Cell. Biochem.* **2004**, *93*, 688-696. doi: 10.1002/jcb.20256.
25. AlQranei, M.S.; Chellaiah, M.A. Osteoclastogenesis in Periodontal Diseases: Possible Mediators and Mechanisms. *J. Oral Biosci.* **2020**, *62*, 123-130. doi: 10.1016/j.job.2020.02.002.
26. Behl, T.; Chadha, S.; Sehgal, A.; Singh, S.; Sharma, N.; Kaur, R.; Bhatia, S.; Al-Harrasi, A.; Chigurupati, S.; Alhowail, A.; Bungau, S. Exploring the Role of Cathepsin in Rheumatoid Arthritis. *Saudi J. Biol. Sci.* **2022**, *29*, 402-410. doi: 10.1016/j.sjbs.2021.09.014.
27. Zhu, X.; Chan, Y.T.; Yung, P.S.H.; Tuan, R.S.; Jiang, Y. Subchondral Bone Remodeling: A Therapeutic Target for Osteoarthritis. *Front. Cell Dev. Biol.* **2021**, *8*, 607764. doi: 10.3389/fcell.2020.607764.
28. Shahryar, N.; Bassam, M. Periprosthetic Osteolysis: Genetics, Mechanisms and Potential Therapeutic Interventions. *Can. J. Surg.* **2012**, *55*, 408. doi: 10.1503/cjs.003711.
29. Hecht, M.; von Metzler, I.; Sack, K.; Kaiser, M.; Sezer, O. Interactions of Myeloma Cells with Osteoclasts Promote Tumour Expansion and Bone Degradation Through Activation of a Complex Signalling Network and Upregulation of Cathepsin K, Matrix Metalloproteinases (MMPs) and Urokinase Plasminogen Activator (uPA). *Exp. Cell Res.* **2008**, *314*, 1082-1093. doi: 10.1016/j.yexcr.2007.10.021.
30. Wang, M.; Xia, F.; Wei, Y.; Wei, X. Molecular Mechanisms and Clinical Management of Cancer Bone Metastasis. *Bone Res.* **2020**, *8*, 30. doi: 10.1038/s41413-020-00105-1.
31. Lindeman, J.H.N.; Hanemaaijer, R.; Mulder, A.; Dijkstra, P.D.S.; Szuhai, K.; Bromme, D.; Verheijen, J.H.; Hogendoorn, P.C.W. Cathepsin K Is the Principal Protease in Giant Cell Tumor of Bone. *Am. J. Pathol.* **2004**, *165*, 593-600. doi: 10.1016/S0002-9440(10)63323-8.
32. Sousa, S.; Clézardin, P. Bone-Targeted Therapies in Cancer-Induced Bone Disease. *Calcif. Tissue Int.* **2018**, *102*, 227-250. doi: 10.1007/s00223-017-0353-5.
33. D'Oronzo, S.; Coleman, R.; Brown, J.; Silvestris, F. Metastatic Bone Disease: Pathogenesis and Therapeutic Options: Up-Date on Bone Metastasis Management. *J. Bone Oncol.* **2019**, *15*, 100205. doi: 10.1016/j.jbo.2018.10.004.

34. Skjødt, M.K.; Frost, M.; Abrahamsen, B. Side Effects of Drugs for Osteoporosis and Metastatic Bone Disease. *Br. J. Clin. Pharmacol.* **2019**, *85*, 1063-1071. doi: 10.1111/bcp.13759.

35. Gralow, J.; Tripathy, D. Managing Metastatic Bone Pain: The Role of Bisphosphonates. *J. Pain Symptom Manage.* **2007**, *33*, 462-472. doi: 10.1016/j.jpainsymman.2007.01.001.

36. Ramaswamy, B.; Shapiro, C.L. Bisphosphonates in the Prevention and Treatment of Bone Metastases. *Oncology (Williston Park N.Y.)* **2003**, *17*, 1261-1270. https://www.cancernetwork.com/view/bisphosphonates-prevention-and-treatment-bone-metastases

37. Littlewood-Evans, A.J.; Bilbe, G.; Bowler, W.B.; Farley, D.; Wlodarski, B.; Kokubo, T.; Inaoka, T.; Sloane, J.; Evans, D.B.; Gallagher, J.A. The Osteoclast-Associated Protease Cathepsin K Is Expressed in Human Breast Carcinoma. *Cancer Res.* **1997**, *57*, 5386-5390.

38. Andrade, S.S.; Gouvea, I.E.; Silva, M.C.C.; Castro, E.D.; de Paula, C.A.A.; Okamoto, D.; Oliveira, L.; Peres, G.B.; Ottaiano, T.; Facina, G.; Nazário, A.C.P.; Campos, A.H.J.F.M.; Paredes-Gamero, E.J.; Juliano, M.; da Silva, I.D.C.G.; Oliva, M.L.V.; Girão, M.J.B.C. Cathepsin K Induces Platelet Dysfunction and Affects Cell Signaling in Breast Cancer - Molecularly Distinct Behavior of Cathepsin K in Breast Cancer. *BMC Cancer* **2016**, *16*, 173. doi: 10.1186/s12885-016-2203-7.

39. Brubaker, K.D.; Vessella, R.L.; True, L.D.; Thomas, R.; Corey, E. Cathepsin K mRNA and Protein Expression in Prostate Cancer Progression. *J. Bone Miner. Res.* **2003**, *18*, 222-230. doi: 10.1359/jbmr.2003.18.2.222.

40. Verbovšek, U.; Motaln, H.; Rotter, A.; Atai, N.A.; Gruden, K.; Van Noorden, C.J.F.; Lah, T.T. Expression Analysis of All Protease Genes Reveals Cathepsin K to Be Overexpressed in Glioblastoma. *PLoS ONE* **2014**, *9*, e111819. doi: 10.1371/journal.pone.0111819.

41. Lisabeth, L.; Bushnell, C. Stroke Risk in Women: The Role of Menopause and Hormone Therapy. *Lancet Neurol.* **2012**, *11*, 82-91. doi: 10.1016/S1474-4422(11)70269-1.

42. Jørgensen, L.; Engstad, T.; Jacobsen, B.K. Bone Mineral Density in Acute Stroke Patients. *Stroke* **2001**, *32*, 47-51. doi: 10.1161/01.STR.32.1.47.

43. Burke, A.P.; Farb, A.; Malcom, G.; Virmani, R. Effect of Menopause on Plaque Morphologic Characteristics in Coronary Atherosclerosis. *Am. Heart J.* **2001**, *141*, S58-S62. doi: 10.1067/mhj.2001.109946.

44. Liang, W.; Wang, F.; Chen, Q.; Dai, J.; Escara-Wilke, J.; Keller, E.T.; Zimmermann, J.; Hong, N.; Lu, Y.; Zhang, J. Targeting Cathepsin K Diminishes Prostate Cancer Establishment and Growth in Murine Bone. *J. Cancer Res. Clin. Oncol.* **2019**, *145*, 1999-2012. doi: 10.1007/s00432-019-02950-y.

45. Le Gall, C.; Bonnelye, E.; Clézardin, P. Cathepsin K Inhibitors as Treatment of Bone Metastasis. *Curr. Opin. Support. Palliat. Care* **2008**, *2*, 218-222. doi: 10.1097/SPC.0b013e32830baea9.

46. Le Gall, C.; Bellahcène, A.; Bonnelye, E.; Gasser, J.A.; Castronovo, V.; Green, J.; Zimmermann, J.; Clézardin, P. A Cathepsin K Inhibitor Reduces Breast Cancer-Induced Osteolysis and Skeletal Tumor Burden. *Cancer Res.* **2007**, *67*, 9894-9902. doi: 10.1158/0008-5472.Can-06-3940.

47. Duong, L.T.; Wesolowski, G.A.; Leung, P.; Oballa, R.; Pickarski, M. Efficacy of a Cathepsin K Inhibitor in a Preclinical Model for Prevention and Treatment of Breast Cancer Bone Metastasis. *Mol. Cancer Ther.* **2014**, *13*, 2898-2909. doi: 10.1158/1535-7163.Mct-14-0253.

48. Jensen, A.B.; Wynne, C.; Ramirez, G.; He, W.; Song, Y.; Berd, Y.; Wang, H.; Mehta, A.; Lombardi, A. The Cathepsin K Inhibitor Odanacatib Suppresses Bone Resorption in Women With Breast Cancer and Established Bone Metastases: Results of a 4-Week, Double-Blind, Randomized, Controlled Trial. *Clin. Breast Cancer* **2010**, *10*, 452-458. doi: 10.3816/CBC.2010.n.059.

49. Law, S.; Andrault, P.-M.; Aguda, A.H.; Nguyen, N.T.; Kruglyak, N.; Brayer, G.D.; Brömme, D. Identification of Mouse Cathepsin K Structural Elements that Regulate the Potency of Odanacatib. *Biochem. J.* **2017**, *474*, 851-864. doi: 10.1042/BCJ20160985.

50. Fantozzi, A.; Christofori, G. Mouse Models of Breast Cancer Metastasis. *Breast Cancer Res.* **2006**, *8*, 212. doi: 10.1186/bcr1530.

51. Behring, L.; Ruiz-Gómez, G.; Trapp, C.; Morales, M.; Wodtke, R.; Köckerling, M.; Kopka, K.; Pisabarro, M.T.; Pietzsch, J.; Löser, R. Dipeptide-Derived Alkynes as Potent and Selective Irreversible Inhibitors of Cysteine Cathepsins. *J. Med. Chem.* **2023**, *66*, 3818-3851. doi: 10.1021/acs.jmedchem.2c01360.

52. Brewitz, L.; Dumjahn, L.; Zhao, Y.; Owen, C.D.; Laidlaw, S.M.; Malla, T.R.; Nguyen, D.; Lukacik, P.; Salah, E.; Crawshaw, A.D.; Warren, A.J.; Trincao, J.; Strain-Damerell, C.; Carroll, M.W.; Walsh, M.A.; Schofield, C.J. Alkyne Derivatives of SARS-CoV-2 Main Protease Inhibitors Including Nirmatrelvir Inhibit by Reacting Covalently with the Nucleophilic Cysteine. *J. Med. Chem.* **2023**, *66*, 2663-2680. doi: 10.1021/acs.jmedchem.2c01627.

53. Ngo, C.; Fried, W.; Aliyari, S.; Feng, J.; Qin, C.; Zhang, S.; Yang, H.; Shanaa, J.; Feng, P.; Cheng, G.; Chen, X.S.; Zhang, C. Alkyne as a Latent Warhead to Covalently Target SARS-CoV-2 Main Protease. *J. Med. Chem.* **2023**, *66*, 12237-12248. doi: 10.1021/acs.jmedchem.3c00810.

54. Di Sarno, V.; Lauro, G.; Musella, S.; Ciaglia, T.; Vestuto, V.; Sala, M.; Scala, M.C.; Smaldone, G.; Di Matteo, F.; Novi, S.; Tecce, M.F.; Moltedo, O.; Bifulco, G.; Campiglia, P.; Gomez-Monterrey, I.M.; Snoeck, R.; Andrei, G.; Ostacolo, C.; Bertamino, A. Identification of a Dual Acting SARS-CoV-2 Proteases Inhibitor Through In Silico Design and Step-By-Step Biological Characterization. *Eur. J. Med. Chem.* **2021**, *226*, 113863. doi: 10.1016/j.ejmech.2021.113863.

55. Tan, B.; Sacco, M.; Tan, H.; Li, K.; Joyce, R.; Zhang, X.; Chen, Y.; Wang, J. Exploring Diverse Reactive Warheads for the Design of SARS-CoV-2 Main Protease Inhibitors. *Eur. J. Med. Chem.* **2023**, *259*, 115667. doi: 10.1016/j.ejmech.2023.115667.

56. Deng, W.; Chen, X.; Jiang, K.; Song, X.; Huang, M.; Tu, Z.-C.; Zhang, Z.; Lin, X.; Ortega, R.; Patterson, A.V.; Smaill, J.B.; Ding, K.; Chen, S.; Chen, Y.; Lu, X. Investigation of Covalent Warheads in the Design of 2-Aminopyrimidine-based FGFR4 Inhibitors. *ACS Med. Chem. Lett.* **2021**, *12*, 647-652. doi: 10.1021/acsmedchemlett.1c00052.

57. Witting, K.F.; van der Heden van Noort, G.J.; Kofoed, C.; Talavera Ormeño, C.; el Atmioui, D.; Mulder, M.P.C.; Ovaa, H. Generation of the UFM1 Toolkit for Profiling UFM1-Specific Proteases and Ligases. *Angew. Chem. Int. Ed.* **2018**, *57*, 14164-14168. doi: 10.1002/anie.201809232.

58. Basters, A.; Geurink, P.P.; Röcker, A.; Witting, K.F.; Tadayon, R.; Hess, S.; Semrau, M.S.; Storici, P.; Ovaa, H.; Knobeloch, K.-P.; Fritz, G. Structural Basis of the Specificity of USP18 Toward ISG15. *Nat. Struct. Mol. Biol.* **2017**, *24*, 270-278. doi: 10.1038/nsmb.3371.

59. Huppelschoten, Y.; Buchardt, J.; Nielsen, T.E.; Sapmaz, A.; van der Heden van Noort, G.J. Total Chemical Synthesis of LC3A and LC3B Activity-Based Probes. *Biomedicines* **2023**, *11*, 884. doi: 10.3390/biomedicines11030884.

60. Gjonaj, L.; Sapmaz, A.; González-Prieto, R.; Vertegaal, A.C.O.; Flierman, D.; Ovaa, H. USP7: Combining Tools towards Selectivity. *Chem. Commun.* **2019**, *55*, 5075-5078. doi: 10.1039/C9CC00969H.

61. Gjonaj, L.; Sapmaz, A.; Flierman, D.; Janssen, G.M.C.; van Veelen, P.A.; Ovaa, H. Development of a DUB-Selective Fluorogenic Substrate. *Chem. Sci.* **2019**, *10*, 10290-10296. doi: 10.1039/C9SC02226K.

62. Hewitt, C.S.; Das, C.; Flaherty, D.P. Rational Development and Characterization of a Ubiquitin Variant with Selectivity for Ubiquitin C-Terminal Hydrolase L3. *Biomolecules* **2022**, *12*, 62. doi: 10.3390/biom12010062.

63. Flierman, D.; van der Heden van Noort, G.J.; Ekkebus, R.; Geurink, P.P.; Mevissen, T.E.T.; Hospenthal, M.K.; Komander, D.; Ovaa, H. Non-hydrolyzable Diubiquitin Probes Reveal Linkage-Specific Reactivity of Deubiquitylating Enzymes Mediated by S2 Pockets. *Cell Chem. Biol. 2016*, *23*, 472-482. doi: 10.1016/j.chembiol.2016.03.009.

64. Hewings, D.S.; Heideker, J.; Ma, T.P.; AhYoung, A.P.; El Oualid, F.; Amore, A.; Costakes, G.T.; Kirchhofer, D.; Brasher, B.; Pillow, T.; Popovych, N.; Maurer, T.; Schwerdtfeger, C.; Forrest, W.F.; Yu, K.; Flygare, J.; Bogyo, M.; Wertz, I.E. Reactive-Site-Centric Chemoproteomics Identifies a Distinct Class of Deubiquitinase Enzymes. *Nat. Commun.* **2018**, *9*, 1162. doi: 10.1038/s41467-018-03511-6.
65. Pinto-Fernández, A.; Davis, S.; Schofield, A.B.; Scott, H.C.; Zhang, P.; Salah, E.; Mathea, S.; Charles, P.D.; Damianou, A.; Bond, G.; Fischer, R.; Kessler, B.M. Comprehensive Landscape of Active Deubiquitinating Enzymes Profiled by Advanced Chemoproteomics. *Front. Chem.* **2019**, *7*, 592. doi: 10.3389/fchem.2019.00592.
66. Nair, R.M.; Seenivasan, A.; Liu, B.; Chen, D.; Lowe, E.D.; Lorenz, S. Reconstitution and Structural Analysis of a HECT Ligase-Ubiquitin Complex via an Activity-Based Probe. *ACS Chem. Biol.* **2021**, *16*, 1615-1621. doi: 10.1021/acschembio.1c00433.
67. Franklin, T.G.; Brzovic, P.S.; Pruneda, J.N. Bacterial Mimicry of Eukaryotic HECT Ubiquitin Ligation. *bioRxiv* **2023**. doi: 10.1101/2023.06.05.543783.
68. Geurink, P.P.; van Tol, B.D.M.; van Dalen, D.; Brundel, P.J.G.; Mevissen, T.E.T.; Pruneda, J.N.; Elliott, P.R.; van Tilburg, G.B.A.; Komander, D.; Ovaa, H. Development of Diubiquitin-Based FRET Probes To Quantify Ubiquitin Linkage Specificity of Deubiquitinating Enzymes. *ChemBioChem* **2016**, *17*, 816-820. doi: 10.1002/cbic.201600017.
69. Miyahisa, I.; Sameshima, T.; Hixon, M.S. Rapid Determination of the Specificity Constant of Irreversible Inhibitors (k_{inact}/K_I) by Means of an Endpoint Competition Assay. *Angew. Chem. Int. Ed.* **2015**, *54*, 14099-14102. doi: 10.1002/anie.201505800.
70. Takeuchi, Y.; Fujiwara, T.; Shimone, Y.; Miyataka, H.; Satoh, T.; Kirk, K.L.; Hori, H. Possible Involvement of Radical Intermediates in the Inhibition of Cysteine Proteases by Allenyl Esters and Amides. *Bioorg. Med. Chem. Lett.* **2008**, *18*, 6202-6205. doi: 10.1016/j.bmcl.2008.10.007.
71. Castarlenas, R.; Di Giuseppe, A.; Pérez-Torrente, J.J.; Oro, L.A. The Emergence of Transition-Metal-Mediated Hydrothiolation of Unsaturated Carbon–Carbon Bonds: A Mechanistic Outlook. *Angew. Chem. Int. Ed.* **2012**, *52*, 211-222. doi: 10.1002/anie.201205468.
72. Dénès, F.; Pichowicz, M.; Povie, G.; Renaud, P. Thiyl Radicals in Organic Synthesis. *Chem. Rev.* **2014**, *114*, 2587-2693. doi: 10.1021/cr400441m.
73. Schöneich, C. Thiyl Radical Reactions in the Chemical Degradation of Pharmaceutical Proteins. *Molecules* **2019**, *24*, 4357. doi: 10.3390/molecules24234357.
74. McLean, J.T.; Benny, A.; Nolan, M.D.; Swinand, G.; Scanlan, E.M. Cysteinyl Radicals in Chemical Synthesis and in Nature. *Chem. Soc. Rev.* **2021**, *50*, 10857-10894. doi: 10.1039/D1CS00254F.
75. Taylor, N.C.; Hessman, G.; Kramer, H.B.; McGouran, J.F. Probing Enzymatic Activity – A Radical Approach. *Chem. Sci.* **2020**, *11*, 2967-2972. doi: 10.1039/C9SC05258E.
76. Hanpude, P.; Bhattacharya, S.; Dey, A.K.; Maiti, T.K. Deubiquitinating Enzymes in Cellular Signaling and Disease Regulation. *IUBMB Life* **2015**, *67*, 544-555. doi: 10.1002/iub.1402.
77. Endres, E.; Chen, N.Y.; Sotriffer, C. MD-Based Assessment of Covalent Inhibitors in Noncovalent Association Complexes: Learning from Cathepsin K as a Test Case. *J. Chem. Inf. Model.* **2023**, *63*, 3186-3197. doi: 10.1021/acs.jcim.3c00061.
78. Dos Santos, A.M.; Oliveira, A.R.S.; da Costa, C.H.S.; Kenny, P.W.; Montanari, C.A.; Varela, J.J.G. Júnior; Lameira, J. Assessment of Reversibility for Covalent Cysteine Protease Inhibitors Using Quantum Mechanics/Molecular Mechanics Free Energy Surfaces. *J. Chem. Inf. Model.* **2022**, *62*, 4083-4094. doi: 10.1021/acs.jcim.2c00466.
79. Voice, A.T.; Tresadern, G.; Twidale, R.M.; van Vlijmen, H.; Mulholland, A.J. Mechanism of Covalent Binding of Ibrutinib to Bruton's Tyrosine Kinase Revealed by QM/MM Calculations. *Chem. Sci.* **2021**, *12*, 5511-5516. doi: 10.1039/D0SC06122K.
80. Quesne, M.G.; Ward, R.A.; De Visser, S.P. Cysteine Protease Inhibition by Nitrile-Based Inhibitors: a Computational Study. *Front. Chem.* **2013**, *1*, 39. doi: 10.3389/fchem.2013.00039.
81. Bonatto, V.; Lameiro, R.F.; Rocho, F.R.; Lameira, J.; Leitão, A.; Montanari, C.A. Nitriles: An Attractive Approach to the Development of Covalent Inhibitors. *RSC Med. Chem.* **2023**, *14*, 201-217. doi: 10.1039/D2MD00204C.
82. Ma, S.; Devi-Kesavan, L.S.; Gao, J. Molecular Dynamics Simulations of the Catalytic Pathway of a Cysteine Protease: A Combined QM/MM Study of Human Cathepsin K. *J. Am. Chem. Soc.* **2007**, *129*, 13633-13645. doi: 10.1021/ja074222+.